

# The Multi-Cluster Fluctuating Two-Ray Fading Model

José David Vega Sánchez, F. Javier López-Martínez, José F. Paris and Juan M. Romero-Jerez

**Abstract**—We introduce a new class of fading channels, built as the superposition of two fluctuating specular components with random phases, plus a clustering of scattered waves: the Multi-cluster Fluctuating Two-Ray (MFTR) fading channel. The MFTR model emerges as a natural generalization of *both* the fluctuating two-ray (FTR) and the  $\kappa$ - $\mu$  shadowed fading models through a more general yet equally mathematically tractable model. This generalization enables the presence of additional multipath clusters in the purely ray-based FTR model, and the convenience of the new underlying fading channel model is discussed in depth. Then, we derive all the chief probability functions of the MFTR model (e.g., probability density function (PDF), cumulative density function (CDF), and moment generation function) in closed-form, having a mathematical complexity similar to other fading models in the state-of-the-art. We also provide two additional analytical formulations for the PDF and the CDF: (i) in terms of a continuous mixture of  $\kappa$ - $\mu$  shadowed distributions, and (ii) as an infinite discrete mixture of Gamma distributions. Such expressions enable to conduct performance analysis under MFTR fading by *directly* leveraging readily available results for the  $\kappa$ - $\mu$  shadowed or Nakagami- $m$  cases, respectively. The performance of wireless communications systems undergoing MFTR fading is exemplified in terms of a classical benchmarking metric like the outage probability, both in exact and asymptotic forms, and the amount of fading.

**Index Terms**—Generalized fading channels, wireless channel modeling, moment generating function, multipath propagation, fluctuating two-ray.

## I. INTRODUCTION

AS radio signals travel along a certain propagation environment, their interaction with objects, system agents and the propagation medium itself causes a number of effects that ultimately determine the amount of power being received at a given location. Classically, these phenomena have been well-characterized through the central limit theorem (CLT), that gives rise to a family of Gaussian models, being the most

popular and widespread-used the Rayleigh/Rician models and also including more general ones like the Hoyt and Beckmann models [1, 2]. While CLT-based models have sufficed to characterize the effects of fading for decades, the rapid growth of wireless technologies along the 21<sup>st</sup> century requires more sophisticated efforts to properly capture the intrinsic nature of wireless propagation as we move up in frequency (where the CLT assumption may no longer hold) [3, 4], or when new use cases demand for improved accuracy, especially in very low-outage regimes [5, 6].

The key advances in wireless fading channel modeling during the last years have been largely based on two different approaches. On the one hand, power envelope-based formulations were used by Yacoub to propose two families of generalized models: the  $\kappa$ - $\mu$  and the  $\eta$ - $\mu$  distributions [7]. These distributions were later generalized and unified through the  $\kappa$ - $\mu$  shadowed fading distribution [8, 9], which has become rather popular in the literature thanks to its ability to model a wide number of propagation conditions through a limited set of physically-justified parameters. On the other hand, ray-based formulations express the received signal as a superposition of a number of scattered waves with random phases [10]. Despite their clear physical motivation, the mathematical complexity associated to ray-based models grows when more than a few dominant waves are individually accounted for [11]. However, Durgin’s Two-Wave with Diffuse Power (TWDP) fading model and its subsequent generalizations [3, 12, 13] have also managed to become popular in the context of wireless channel modeling for higher-frequency bands. Specifically, the Fluctuating Two-Ray (FTR) fading model [3] has enthusiastically been adopted in mm-Wave environments, and even recently in terahertz (THz) bands [14].

Key to their success, the  $\kappa$ - $\mu$  shadowed and the FTR fading models share a number of features that are desirable for a stochastic fading model to be of practical use: (i) have a small number (three, in both cases) of physically justified parameters; (ii) have a reasonably good mathematical tractability; (iii) include simpler but popular fading models as special cases. However, because these two models arise from different physical formulations, they do not capture the same type of propagation behaviors. For instance, the FTR model has the ability to exhibit bimodality that often appears in field measurements [14–16], while the  $\kappa$ - $\mu$  shadowed one is inherently unimodal in its original formulation [8]. On the other hand, the  $\kappa$ - $\mu$  shadowed model can exhibit any sort of power-law asymptotic decay (diversity order), while ray-based models asymptotically decay with unitary slope [11].

Aiming to reconcile the two dominant approaches in the

This work was submitted to the IEEE for publication on May 31, 2022. Copyright may be transferred without notice, after which this version may no longer be accessible. Manuscript received MONTH xx, YEAR; revised XXX. The review of this paper was coordinated by XXXX. The work of F. J. López-Martínez, J. F. Paris and J. M. Romero-Jerez was funded in part by Junta de Andalucía, the European Union and the European Fund for Regional Development FEDER through grants P18-RT-3175 and EMERGIA20-00297, and in part by MCIN/AEI/10.13039/501100011033 through grant PID2020-118139RB-I00. (Corresponding author: Juan M. Romero-Jerez)

J. D. Vega Sánchez is with the Departamento de Electrónica, Telecomunicaciones y Redes de Información, Escuela Politécnica Nacional (EPN), Quito, 170525, Ecuador. (E-mail: jose.vega01@epn.edu.ec)

F. J. López-Martínez, J. F. Paris and J. M. Romero-Jerez are with the Communications and Signal Processing Lab, Telecommunication Research Institute (TELMA), Universidad de Málaga, Málaga, 29010, (Spain). F. J. López-Martínez is also with the Dept. Signal Theory, Networking and Communications, University of Granada, 18071, Granada (Spain). (E-mails: fjlm@ugr.es, paris@ic.uma.es, romero@dte.uma.es)

literature of stochastic fading channel modeling, which have hitherto evolved separately, we here introduce the Multi-cluster Fluctuating Two-Ray (MFTR) fading model. This newly proposed model is presented as the natural generalization and unification of *both* the FTR and the  $\kappa$ - $\mu$  shadowed fading models. Such generalization enables the presence of additional multipath clusters in the purely ray-based FTR model, and the consideration of two fluctuating specular components within  $\kappa$ - $\mu$  shadowed formulation. Despite being a generalization of the FTR and the  $\kappa$ - $\mu$  shadowed models, only one additional parameter is required over these baseline models. As we will later see, the MFTR model not only inherits the bimodality and asymptotic decay properties exhibited separately by the FTR and  $\kappa$ - $\mu$  shadowed models, respectively, but also brings out additional flexibility to model propagation features not captured by the models from which it is originated. The resulting formulations of the MFTR statistics are as tractable as those of the simpler baseline models, and of other fading models in the state-of-the-art. The key contributions of this work can be listed as follows:

- We derive the chief probability functions for the MFTR model, i.e., probability density function (PDF), cumulative density function (CDF), and moment generation function (MGF) in closed-form. These expressions allow for the computation of the MFTR statistics using special functions similar to those used in simpler, well-established fading models such as Rician shadowed [17],  $\kappa$ - $\mu$  shadowed [8], or FTR [3].
- Aiming to facilitate the use of the MFTR fading model for performance analysis purposes, we provide two alternative analytical formulations for the PDF and the CDF: one in terms of a continuous mixture of  $\kappa$ - $\mu$  shadowed distributions, and another one as an infinite discrete mixture of Gamma distributions. This allows to leverage the rich literature of performance analysis, so that existing results available either for the  $\kappa$ - $\mu$  shadowed or the Nakagami- $m$  cases can be used as a starting point to *straightforwardly* analyze the performance under MFTR fading.
- These results are used to analyze the outage probability performance under MFTR fading, both in exact and asymptotic form, and to study the impact of the model parameters on the amount of fading (AoF) metric.

The remainder of this paper is organized as follows: preliminaries and channel models are described in Section II. In Section III, analytical expressions are derived for the main statistics of the MFTR model. In Section IV, performance analysis over MFTR fading channels is exemplified. Section V shows illustrative numerical results and discussions. Finally, concluding remarks are provided in Section VI.

*Notation:* In what follows,  $f_{(\cdot)}(\cdot)$  and  $F_{(\cdot)}(\cdot)$  denote the PDF and CDF, respectively;  $\mathbb{E}\{\cdot\}$  and  $\mathbb{V}\{\cdot\}$  are the expectation and variance operators;  $\Pr\{\cdot\}$  represents probability;  $|\cdot|$  is the absolute value,  $\simeq$  refers to ‘‘asymptotically equal to’’,  $\equiv$  reads as ‘‘is equivalent to’’,  $\approx$  denotes ‘‘approximately equal to’’ and  $\sim$  refers to ‘‘statistically distributed as’’. In addition,  $\Gamma(\cdot)$  denotes the gamma function [18, Eq. (6.1.1)],  $\gamma(\cdot, \cdot)$  is the lower

incomplete gamma function [18, Eq. (6.5.2)],  $(a)_n = \frac{\Gamma(a+n)}{\Gamma(a)}$  represents the Pochhammer’s symbol [18],  ${}_2F_1(\cdot, \cdot; \cdot; \cdot)$  is the Gauss hypergeometric function [18, Eq. (15.1.1)],  $P_\alpha(z) = {}_2F_1(-\alpha, \alpha + 1; 1; \frac{1-z}{2})$  is the Legendre function of the first kind of real degree  $\alpha$  [18, Eq. (8.1.2)],  $\Phi_2^{(4)}(\cdot, \cdot, \cdot, \cdot; \cdot, \cdot, \cdot, \cdot)$  denotes the confluent hypergeometric function in four variables [19, Eq. (8)], and  $\Phi_2(\cdot, \cdot; \cdot, \cdot; \cdot, \cdot)$  is the bivariate confluent hypergeometric function [20, Eq. (4.19)].

## II. PRELIMINARIES AND CHANNEL MODELS

According to [12], the small-scale random fluctuations of a radio signal transmitted over a wireless channel can be structured at the receiver as a superposition of  $N$  waves arising from dominant specular components, plus a group of multipath waves associated to diffuse scattering. Therefore, under this model, the received complex baseband signal representing the wireless channel can be expressed as

$$V_r = \sum_{n=1}^N V_n \exp(j\phi_n) + X_1 + jY_1, \quad (1)$$

where  $V_n \exp(j\phi_n)$  denotes the  $n$ th specular component with constant amplitude  $V_n$  and uniformly distributed random phase  $\phi_n \sim \mathcal{U}(0, 2\pi)$ . On the other hand,  $X_1 + jY_1$  is a circularly-symmetric complex Gaussian random variable (RV) with total power  $2\sigma^2$ , such that  $X_1, Y_1 \sim \mathcal{N}(0, \sigma^2)$ , representing the scattering components associated to the non-line-of-sight (NLOS) propagation. This model allows to individually account for a number of dominant waves, together with the application of the CLT to the diffuse component, where a sufficiently large number of weak diffuse waves with independent phases is assumed.

The FTR channel model was proposed in [3] as a generalization of the TWDP model [12], where the latter arises when considering two dominant specular components (i.e.,  $N = 2$ ) in (1). For its definition, the FTR model considers that the amplitudes of these two dominant components experience a joint fluctuation due to the natural situations in different wireless scenarios (e.g., human body shadowing do to user motion, electromagnetic disturbances, and many others). Based on this, the complex signal under FTR fading can be formulated as [3]

$$V_{\text{FTR}} = \sqrt{\zeta} V_1 \exp(j\phi_1) + \sqrt{\zeta} V_2 \exp(j\phi_2) + X_1 + jY_1, \quad (2)$$

where  $\zeta$  is a unit-mean Gamma distributed RV whose PDF is given by

$$f_\zeta(x) = \frac{m^m x^{m-1}}{\Gamma(m)} \exp(-mx), \quad (3)$$

where  $m$  denotes the shadowing severity index of the specular components, often linked to line-of-sight (LOS) propagation. Note that when  $m \rightarrow \infty$ , then  $\zeta$  degenerates into a deterministic value and the amplitudes of the two dominant specular components in (2) become constant. The FTR model in (2), besides fitting well with the field measurements in different wireless scenarios, also encompasses important statistical wireless channel models as particular cases. For instance, when no LOS components are present in (2), i.e.,  $N = 0$ ,

the classical Rayleigh fading model arises. For a single LOS component, i.e.,  $N = 1$ , two fading models are obtained, namely, Rician and Rician shadowed [17] for constant and fluctuating amplitudes, respectively. Finally, for the case in which there are two dominant components (i.e.,  $N = 2$ ) with constant amplitudes, (2) reduces to the TWDP fading model, also referred to as the Generalized Two-Ray fading model with uniformly distributed phases (GTR-U) [13].

On the other hand, power-envelope based formulations as those originally proposed by Yacoub [7] are defined from a different approach. Specifically, the squared amplitude (or instantaneous received power) of the  $\kappa$ - $\mu$  shadowed fading model is expressed as [8]

$$R^2 = \sum_{i=1}^{\mu} |Z_i + \sqrt{\zeta} p_i|^2, \quad (4)$$

where  $\mu$  wave clusters are defined, the complex variables  $Z_i$  denote the diffuse components associated to each cluster,  $\zeta$  is a unit-mean Gamma distributed RV, as given in (3), and  $p_i$  are complex amplitudes for the dominant components within each cluster. Notice that the FTR model in (2) can be physically interpreted as a single cluster in which both LOS and NLOS components are part of the same cluster structure. With this in mind, we can combine a power-envelope definition as the one in (4) with the ray-based structure in (2) as follows.

As in [7], we consider a wireless signal composed of clusters of waves propagating in a non-homogeneous environment. Within each cluster, the scattered waves have random phases and similar delay times, while the intercluster delay-time spreads are assumed to be relatively large. All clusters of the multipath waves are assumed to have scattered waves with identical powers. Now, in the first cluster (which typically represents the first one arriving), two dominant specular components with random phases and arbitrary power are considered, whereas  $p_i = 0, \forall i = 2 \dots \mu$ . Similarly to the model in [3], these dominant components are subject to the same source of random fluctuations. Under this channel model, the squared amplitude of the received signal is expressed as

$$R^2 = \underbrace{|\sqrt{\zeta} (V_1 e^{j\phi_1} + V_2 e^{j\phi_2}) + X_1 + jY_1|^2}_{\text{cluster 1: } V_{\text{FTR}}} + \underbrace{\sum_{i=2}^{\mu} |Z_i|^2}_{\text{additional clusters}} \quad (5)$$

where  $Z_i = X_i + jY_i$ , for  $i = \{2, \dots, \mu\}$  in which  $X_i$  and  $Y_i$  are mutually independent zero-mean Gaussian processes with  $\sigma^2$  variance, i.e.,  $\mathbb{E}\{X_i^2\} = \mathbb{E}\{Y_i^2\} = \sigma^2$ . The insightful interpretation of (5) is the following. Each additional multipath cluster is modelled by one term of the sum; thus,  $\mu$  is the total number of multipath clusters. The scattered components (e.g., NLOS waves) of the  $i$ th cluster are denoted by a circularly-symmetric complex Gaussian RV, i.e.,  $Z_i$ . Hence, for the  $i$ th cluster, the total power of the scattered multipath signals is  $2\sigma^2$ . Moreover, in cluster 1, the complex RVs represented by  $V_n \exp(j\phi_n)$ , for  $n = \{1, 2\}$  denote the dominant specular components (e.g., LOS waves) of the first arriving cluster. Finally, the two specular components in cluster 1 are subject to the same source of random fluctuations as in the original

FTR model, denoted by the normalized RV  $\zeta$ . For the model in (5), we coin the name multicluster FTR (MFTR) model, to indicate the presence of additional multipath clusters in the original FTR model.

It must be noted that the statistical formulation of the  $\kappa$ - $\mu$  shadowed distribution depends (through parameter  $\kappa$ ) on the total aggregate power of the specular components, but it is independent of which or how many clusters incorporate a specular component [8]; therefore, the MFTR model defined in (5) fully includes *both* the original FTR model and the  $\kappa$ - $\mu$  shadowed distribution as special cases. Both models have independently been validated, empirically matching different wireless scenarios [3, 8], which guarantees the practical usefulness of the proposed MFTR model.

As in [7, 8], even though the cluster number  $\mu$  is inherently a natural number, the MFTR model admits a generalization for  $\mu \in \mathbb{R}^+$ , which is considered in the subsequent derivations.

### III. STATISTICAL CHARACTERIZATION OF THE MFTR FADING MODEL

In this section, the key first-order statistics of the newly proposed MFTR model are derived: the MGF, PDF and CDF. In the following derivations, let us consider the received power signal of the MFTR model, i.e.,  $W = R^2$ , which from (5) can be rewritten as

$$W = \left( \sqrt{\zeta} (V_1 \cos \phi_1 + V_2 \cos \phi_2) + X_1 \right)^2 + \left( \sqrt{\zeta} (V_1 \sin \phi_1 + V_2 \sin \phi_2) + Y_1 \right)^2 + \sum_{i=2}^{\mu} X_i^2 + Y_i^2. \quad (6)$$

As in [3], the MFTR model can be conveniently expressed by introducing the parameters  $K$  and  $\Delta$ , which are respectively defined as

$$K = \frac{V_1^2 + V_2^2}{2\sigma^2\mu}, \quad (7)$$

$$\Delta = \frac{2V_1V_2}{V_1^2 + V_2^2}. \quad (8)$$

The MFTR fading model is univocally defined by four shape parameters:  $\{K, m, \mu\} \in \mathbb{R}^+$  and  $\Delta \in [0, 1]$ . Similar to the interpretation of the Rician  $K$  factor,  $K$  represents the ratio of the average power of the specular components to the power of the remaining scattered components. On the other hand, the  $\Delta$  parameter ranging from 0 to 1 shows how similar to each other are the average received powers of the dominant components in cluster 1. For instance, when the magnitudes of two components are equal,  $\Delta = 1$ . In the absence of a second component ( $V_1$  or  $V_2 = 0$ ),  $\Delta = 0$ , which corresponds to the  $\kappa$ - $\mu$  shadowed model. Furthermore, notice that for  $\mu = 1$  the MFTR model yields the FTR fading model.

Next, we introduce the distribution of the received power signal (or equivalently the instantaneous signal-to-noise ratio (SNR) when the noise comes into play) of the MFTR fading model. It is worth mentioning that the statistical characterization of the instantaneous received SNR, here denoted by  $\gamma$ , plays a pivotal role in designing or evaluating the performance



of many practical wireless systems. Let  $\gamma \triangleq \bar{\gamma}W/\Omega$  be the instantaneous received SNR through the MFTR fading channel, where  $\bar{\gamma}$  and  $\Omega$  denote the average SNR and the mean of  $W$ , respectively. Mathematically speaking, from (6),  $\bar{\gamma}$  can be formulated as

$$\begin{aligned}\bar{\gamma} &= \frac{\bar{\gamma}}{\Omega} \mathbb{E}\{W\} = \frac{\bar{\gamma}}{\Omega} (V_1^2 + V_2^2 + 2\sigma^2\mu) \\ &= \frac{\bar{\gamma}}{\Omega} 2\sigma^2\mu(1+K).\end{aligned}\quad (9)$$

With the aid of the previous definitions, the chief probability functions concerning the MFTR channel model can be derived as follows.

#### A. MGF

In the first Lemma, presented below, we obtain a closed-form expression for the MGF.

**Lemma 1.** *The MGF of the instantaneous received SNR  $\gamma$  under MFTR fading can be expressed as*

$$\begin{aligned}\mathcal{M}_\gamma(s) &= \frac{m^m \mu^\mu (1+K)^\mu (\mu(1+K) - \bar{\gamma}s)^{m-\mu}}{\left(\sqrt{\mathcal{R}(\mu, m, K, \Delta; s)}\right)^m} \\ &\quad \times P_{m-1}\left(\frac{m\mu(1+K) - (\mu K + m)\bar{\gamma}s}{\sqrt{\mathcal{R}(\mu, m, K, \Delta; s)}}\right)\end{aligned}\quad (10)$$

where  $\mathcal{R}(\mu, m, K, \Delta; s)$  is a polynomial in  $s$  given by

$$\begin{aligned}\mathcal{R}(\mu, m, K, \Delta; s) &= \left[(m + \mu K)^2 - (\mu K \Delta)^2\right] \bar{\gamma}^2 s^2 - 2m\mu \\ &\quad \times (1+K)(m + \mu K)\bar{\gamma}s + [(1+K)m\mu]^2.\end{aligned}\quad (11)$$

*Proof.* See Appendix A.  $\square$

Note that the result in Lemma 1 is valid for any positive real value of  $m$ .

#### B. PDF and CDF

Here, we derive the PDF and CDF of the SNR of the MFTR model<sup>1</sup>. Even though these can be computed by performing a numerical Laplace inverse transform over the MGF in Lemma 1 for any arbitrary set of values of the shape parameters [1], it is possible to obtain closed-form expressions by assuming that the fading parameter  $m$  takes integer values. For this purpose, we take advantage of the fact that, for  $m \in \mathbb{Z}^+$ , the Legendre function in the MGF obtained in (10) has an integer degree; thus, such Legendre function becomes a Legendre polynomial. The Legendre polynomial of an integer degree  $n$  can be formulated as in [18, Eq. (22.3.8)] by

$$P_n(z) = \frac{1}{2^n} \sum_{q=0}^{\lfloor n/2 \rfloor} (-1)^q C_q^n z^{n-2q}, \quad (12)$$

<sup>1</sup>The PDF and CDF of the received signal envelope  $R$  under MFTR channels can be obtained through a standard variable transformation. Specifically, by performing the change of variables,  $f_R(r) = 2rf_\gamma(r^2)$  and  $F_R(r) = F_\gamma(r^2)$ , with  $\bar{\gamma}$  replaced by  $\Omega = \mathbb{E}\{R^2\}$ .

where the  $C_q^n$  term is expressed as

$$C_q^n = \binom{n}{q} \binom{2n-2q}{n} = \frac{(2n-2q)!}{q!(n-q)!(n-2q)!}. \quad (13)$$

From the MGF in (10) and with the help of (12), the closed-form expressions for the PDF and CDF of the RV  $\gamma$  are obtained in the following Lemma.

**Lemma 2.** *Assuming that  $m \in \mathbb{Z}^+$ , the PDF and CDF of the SNR under MFTR fading can be formulated as (14) and (15), respectively.*

*Proof.* See Appendix B-A.  $\square$

The chief statistics of the MFTR fading model in (14) and (15) are given in terms of the multi-variate confluent hypergeometric function  $\Phi_2^{(4)}(\cdot)$ , which is rather common in well-established fading models such as Rician shadowed [17],  $\kappa$ - $\mu$  shadowed [8], or FTR [3]. Moreover, the computation of this function can be performed by resorting to an inverse Laplace transform as described in [1, Appendix 9B], and whose implementation in a simple and efficient way through MATLAB is given in [21]. Therefore, the evaluation of MFTR probability distributions does not pose any additional challenge compared to other well-known fading models in the state-of-the-art.

#### C. Alternative formulations

Expressions in Lemmas 1 and 2 provide a complete formulation for the MFTR, equivalent in complexity to those originally proposed in [3] and [8] for the baseline FTR and  $\kappa$ - $\mu$  shadowed fading distributions, respectively. However, aiming to provide additional flexibility to the newly proposed MFTR model, as well as to facilitate its use for performance evaluation purposes, we now provide two alternative formulations for the PDF and CDF of the MFTR model.

We first propose a formulation of the MFTR model as a *continuous* mixture of  $\kappa$ - $\mu$  shadowed distributions. Secondly, we propose a formulation of the MFTR model as an infinite *discrete* mixture of Gamma distributions. These formulations are provided in the following two lemmas, and are valid for the entire range of values of the shape parameters  $\kappa, \mu, m$  and  $\Delta$ .

**Lemma 3.** *When  $m \in \mathbb{R}^+$ , the PDF and CDF of the SNR of the MFTR distribution can be obtained by averaging the conditional  $\kappa$ - $\mu$  shadowed statistics over all possible realizations of  $\theta$ , as*

$$f_\gamma(x) = \frac{1}{\pi} \int_0^\pi f_{\gamma|\theta}(x) d\theta, \quad (20)$$

$$F_\gamma(x) = \frac{1}{\pi} \int_0^\pi F_{\gamma|\theta}(x) d\theta, \quad (21)$$

$$\begin{aligned}
f_\gamma(x) &= \frac{(1+K)^\mu \mu^\mu}{2^{m-1} \Gamma(\mu) \bar{\gamma}^\mu} \left( \frac{m}{\sqrt{(m+\mu K)^2 - \mu^2 K^2 \Delta^2}} \right)^m \sum_{q=0}^{\lfloor \frac{m-1}{2} \rfloor} (-1)^q C_q^{m-1} \left( \frac{m+\mu K}{\sqrt{(m+\mu K)^2 - \mu^2 K^2 \Delta^2}} \right)^{m-1-2q} \\
&\times x^{\mu-1} \Phi_2^{(4)} \left( 1+2q-m, m-q-1/2, m-q-1/2, \mu-m; \mu; -\frac{(1+K)m\mu}{(m+\mu K)\bar{\gamma}}x, -\frac{(1+K)m\mu}{(m+\mu K(1+\Delta))\bar{\gamma}}x, \right. \\
&\quad \left. -\frac{(1+K)m\mu}{(m+\mu K(1-\Delta))\bar{\gamma}}x, -\frac{(1+K)\mu}{\bar{\gamma}}x \right). \tag{14}
\end{aligned}$$

$$\begin{aligned}
F_\gamma(x) &= \frac{(1+K)^\mu \mu^\mu}{2^{m-1} \Gamma(\mu+1) \bar{\gamma}^\mu} \left( \frac{m}{\sqrt{(m+\mu K)^2 - \mu^2 K^2 \Delta^2}} \right)^m \sum_{q=0}^{\lfloor \frac{m-1}{2} \rfloor} (-1)^q C_q^{m-1} \left( \frac{m+\mu K}{\sqrt{(m+\mu K)^2 - \mu^2 K^2 \Delta^2}} \right)^{m-1-2q} \\
&\times x^\mu \Phi_2^{(4)} \left( 1+2q-m, m-q-1/2, m-q-1/2, \mu-m; \mu+1; -\frac{(1+K)m\mu}{(m+\mu K)\bar{\gamma}}x, -\frac{(1+K)m\mu}{(m+\mu K(1+\Delta))\bar{\gamma}}x, \right. \\
&\quad \left. -\frac{(1+K)m\mu}{(m+\mu K(1-\Delta))\bar{\gamma}}x, -\frac{(1+K)\mu}{\bar{\gamma}}x \right). \tag{15}
\end{aligned}$$

$$f_\gamma(x) = \sum_{i=0}^{\infty} w_i f_X^G \left( \mu+i; \frac{\bar{\gamma}(\mu+i)}{\mu(K+1)}; x \right). \tag{16}$$

$$F_\gamma(x) = \sum_{i=0}^{\infty} w_i F_X^G \left( \mu+i; \frac{\bar{\gamma}(\mu+i)}{\mu(K+1)}; x \right). \tag{17}$$

$$\begin{aligned}
w_i &= \frac{\Gamma(m+i)(\mu K)^i m^m}{\Gamma(m)\Gamma(i+1)} \frac{(1-\Delta)^i}{\sqrt{\pi}(\mu K(1-\Delta)+m)^{m+i}} \sum_{q=0}^i \binom{i}{q} \frac{\Gamma(q+\frac{1}{2})}{\Gamma(q+1)} \left( \frac{2\Delta}{1-\Delta} \right)^q \\
&\quad \times {}_2F_1 \left( m+i, q+\frac{1}{2}; q+1; \frac{-2\mu K \Delta}{\mu K(1-\Delta)+m} \right), \quad m \in \mathbb{R}^+, \tag{18}
\end{aligned}$$

$$f_X^G(\lambda; \nu; y) = \frac{\lambda^\lambda}{\Gamma(\lambda)\nu^\lambda} y^{\lambda-1} \exp\left(-\frac{\lambda y}{\nu}\right), \quad F_X^G(\lambda; \nu; y) = \frac{1}{\Gamma(\lambda)} \gamma\left(\lambda, \frac{\lambda y}{\nu}\right). \tag{19}$$

where

$$\begin{aligned}
f_{\gamma|\theta}(x) &= \frac{\mu^\mu m^m (1+K)^\mu}{\Gamma(\mu) \bar{\gamma} (\mu K (1+\Delta \cos \theta) + m)^m} \left( \frac{x}{\bar{\gamma}} \right)^{\mu-1} \\
&\times e^{-\frac{\mu(1+K)}{\bar{\gamma}}x} {}_1F_1 \left( m; \mu; \frac{\mu^2 K (1+\Delta \cos \theta) (1+K) x}{\mu K (1+\Delta \cos \theta) + m \bar{\gamma}} \right), \tag{22}
\end{aligned}$$

$$\begin{aligned}
F_{\gamma|\theta}(x) &= \frac{\mu^{\mu-1} m^m (1+K)^\mu}{\Gamma(\mu) (\mu K (1+\Delta \cos \theta) + m)^m} \left( \frac{x}{\bar{\gamma}} \right)^\mu \Phi_2 \left( \mu-m, \right. \\
&\quad \left. m; \mu+1; -\frac{\mu(1+K)x}{\bar{\gamma}}, -\frac{\mu(1+K)}{\bar{\gamma}} \right) \\
&\quad \times \frac{mx}{\mu K (1+\Delta \cos \theta) + m}. \tag{23}
\end{aligned}$$

*Proof.* The conditional  $\kappa$ - $\mu$  shadowed PDF and CDF are obtained from [8, Eq. (4)] and [8, Eq. (6)] by substituting  $\kappa$  and  $\bar{\gamma}$  by (33) and (34), respectively. Then, using the relationships given in (36) and (39) that connect the  $\kappa$ - $\mu$  shadowed and MFTR models, (22) and (23) are obtained.  $\square$

It must be noted that the Rician shadowed distribution is a particular case of the  $\kappa$ - $\mu$  shadowed distribution for the case when  $\mu = 1$ . Thus, the integral connection between the FTR and the Rician shadowed distributions presented in [22], for arbitrary positive real  $m$ , is a particular case of Lemma 3 for  $\mu = 1$ .

**Lemma 4.** *When  $m \in \mathbb{R}^+$ , the PDF and CDF of the SNR of the MFTR distribution can be obtained as an infinite discrete mixture of Gamma distributions. The corresponding expressions are given in equations (16) and (17), respectively, where  $f_X^G(\cdot)$  and  $F_X^G(\cdot)$  represent the PDF and CDF, respectively, of a Gamma distribution, which are both given in (19). Note that  $\gamma(\cdot, \cdot)$  in (19) represents the incomplete gamma function defined in [18, Eq. (6.5.2)].*

*Proof.* See Appendix B-B.  $\square$

Here, we point out that the PDFs and CDFs in Lemmas 3 and 4 are valid for non-constrained fading values of the MFTR model. Expressions in Lemma 3, i.e., (20) and (21), are expressed in simple finite-integral form in terms of well-known

TABLE I  
CONVENTIONAL AND GENERALIZED FADING CHANNEL MODELS DERIVED  
FROM THE MFTR DISTRIBUTION.

Fading Distribution	MFTR fading parameters
One-sided Gaussian	a) $\underline{\Delta} = 0, \underline{K} \rightarrow \infty, \underline{m} = 0.5, \underline{\mu} = 1$ b) $\underline{\Delta} = 1, \underline{K} \rightarrow \infty, \underline{m} = 1, \underline{\mu} = 1$
Rayleigh	a) $\underline{\Delta} = 0, \underline{K} \rightarrow \infty, \underline{m} = 1, \underline{\mu} = 1$ b) $\underline{\Delta} = 0, \underline{K} = 0, \forall \underline{m}, \underline{\mu} = 1$
Nakagami- $q$ (Hoyt)	a) $\underline{\Delta} = 0, \underline{K} = \frac{1-q^2}{2q^2}, \underline{m} = 0.5, \underline{\mu} = 1$ b) $\forall \{\underline{\Delta}, \underline{K}\}$ , with $q = \sqrt{\frac{1+K(1-\underline{\Delta})}{1+K(1+\underline{\Delta})}}$ , $\underline{m} = 1, \underline{\mu} = 1$
Nakagami- $m$	$\underline{\Delta} = 0, \underline{K} \rightarrow \infty, \underline{m} = m, \underline{\mu} = 1$
Rician	$\underline{\Delta} = 0, \underline{K} = K, \underline{m} \rightarrow \infty, \underline{\mu} = 1$
Rician shadowed	$\underline{\Delta} = 0, \underline{K} = K, \underline{m} = m, \underline{\mu} = 1$
$\kappa$ - $\mu$ shadowed	$\underline{\Delta} = 0, \underline{K} = \kappa, \underline{m} = m, \underline{\mu} = \mu$
$\kappa$ - $\mu$	$\underline{\Delta} = 0, \underline{K} = \kappa, \underline{m} \rightarrow \infty, \underline{\mu} = \mu$
$\eta$ - $\mu$	$\underline{\Delta} = 0, \underline{K} = (1-\eta)/(2\eta), \underline{m} = \mu, \underline{\mu} = 2\mu$
TWDP	$\underline{\Delta} = \underline{\Delta}, \underline{K} = K, \underline{m} \rightarrow \infty, \underline{\mu} = 1$
Two-Wave	$\underline{\Delta} = \underline{\Delta}, \underline{K} \rightarrow \infty, \underline{m} \rightarrow \infty, \underline{\mu} = 1$
FTR	$\underline{\Delta} = \underline{\Delta}, \underline{K} = K, \underline{m} = m, \underline{\mu} = 1$
Fluctuating Two-Wave	$\underline{\Delta} = \underline{\Delta}, \underline{K} \rightarrow \infty, \underline{m} = m, \underline{\mu} = 1$

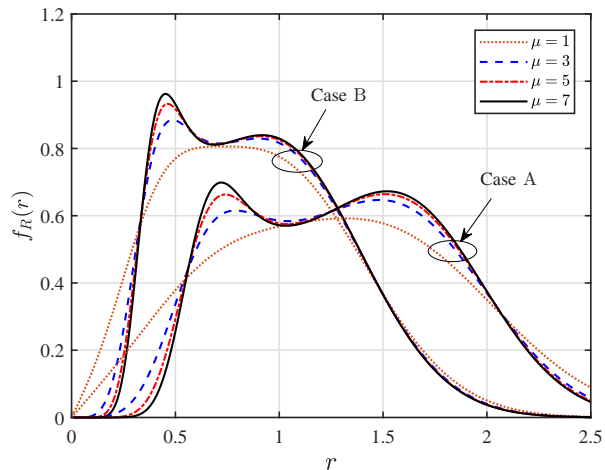


Fig. 1. PDF of the MFTR signal envelope by varying  $\mu$  in two different scenarios: Case A:  $\underline{\Delta} = 0.9, m = 8, K = 8, \bar{\gamma} = 2$  and Case B:  $\underline{\Delta} = 0.9, m = 4, K = 15, \bar{\gamma} = 1$ .

functions in communication theory, where the integrands are continuous bounded functions and the integration interval is finite. Therefore, the evaluation of these integrals through numerical integration routines in commercial mathematical software packages poses no challenge, and in fact is an standard approach in communication theory – cfr. the proper integral forms of the Gaussian  $Q$ -function [23], or Simon and Alouini’s MGF approach to the performance analysis of wireless communication systems [1]. Expressions in Lemma 4, i.e., (16) and (17), are given as weighted sums of gamma distributions, which are a basic building block in many communication theory applications, and correspond to the case of assuming Nakagami- $m$  fading. These sets of expressions allow for leveraging the rich literature devoted to study baseline fading models like  $\kappa$ - $\mu$  shadowed and Nakagami- $m$ , to directly evaluate the case of the more general MFTR model, when desired.

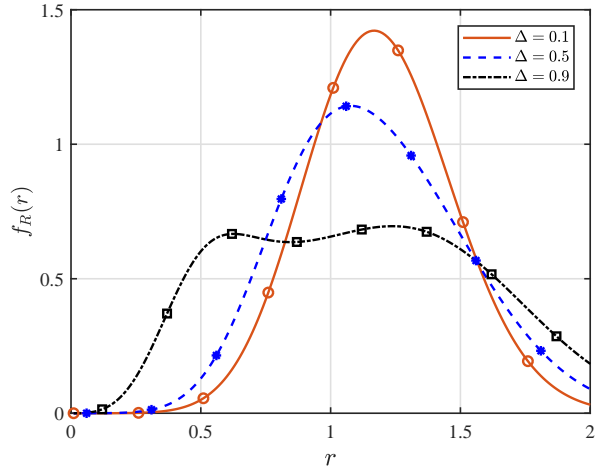


Fig. 2. PDF of the MFTR signal envelope for different values of  $\Delta$ , with  $\mu = 2, m = 6, K = 15$ , and  $\bar{\gamma} = 1.5$ . Markers correspond to MC simulations.

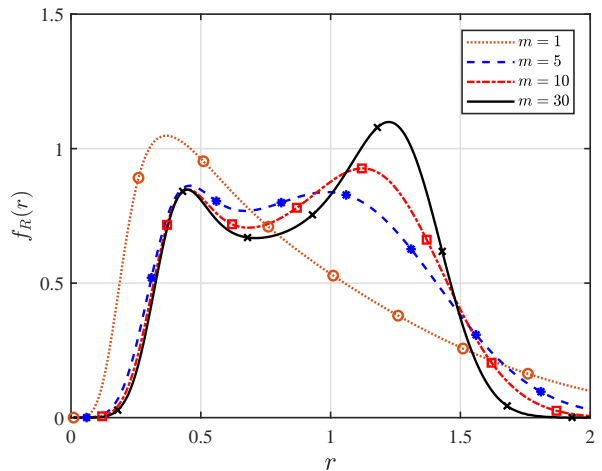


Fig. 3. PDF of the MFTR signal envelope for different values of  $m$ , with  $\Delta = 0.9, \mu = 3, m = 4, K = 20$ , and  $\bar{\gamma} = 1$ . Markers correspond to MC simulations.

#### D. Special cases and effect of parameters

The MFTR model derived here is connected to other fading distributions commonly used in several wireless application scenarios, by specializing the corresponding set of parameters as stated in Table I. In order to avoid confusion, the parameters related to the MFTR distribution are underlined. We would like to mention that a multicluster version of the TWDP model in [12, 13] naturally appears as we let  $m \rightarrow \infty$ ; however, this model alone has its own entity and deserves special attention as a separate item, which is left for future research activities.

In Figs. 1-4, we illustrate how different propagation conditions affect the shape of the MFTR distribution, by evaluating the PDF of the received signal envelope  $f_R(r)$  for a set of values of the shape parameters:  $K$  (power ratio between dominant and diffuse components),  $\Delta$  (amplitude imbalance between the two dominant components),  $m$  (severity of dominant waves’ fluctuation), and  $\mu$  (clustering of scattered multipath waves).

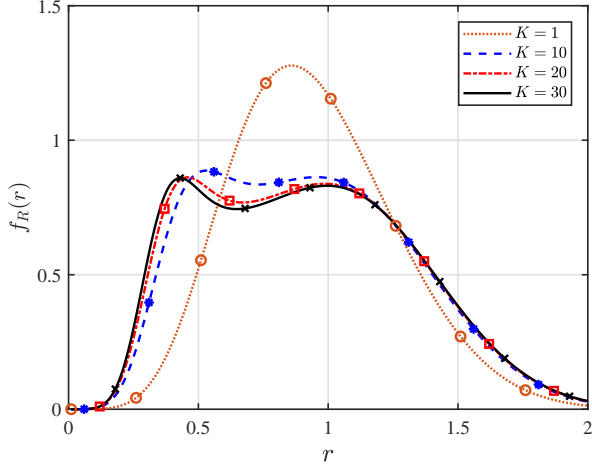


Fig. 4. PDF of the MFTR signal envelope for different values of  $K$ , with  $m = 5$ ,  $\Delta = 0.9$ ,  $\mu = 3$ , and  $\bar{\gamma} = 1$ . Markers correspond to MC simulations

The PDFs illustrated in the figures have been obtained by evaluating (14), although all mathematical expressions along this section have been double-checked through Monte Carlo (MC) simulations. These MC simulations are also included with markers in the figures, whenever they don't affect the readability of the figures. Also, we also checked that the same results are obtained when eqs. (16) and (20) are used to evaluate the PDFs.

In Fig. 1, we clearly perceive that the MFTR model's behavior is inherently bimodal<sup>2</sup> (see *Case A*). Interestingly, thanks to the presence of the  $\mu$  parameter adequately combined with the other fading parameters, the MFTR model can exhibit a more pronounced bimodality as  $\mu$  increases (see *Case B*). Specifically, the MFTR model can exhibit both a left-bimodality (i.e., the first local maximum is larger) and a right-bimodality (i.e., the second local maximum is larger). This is in stark contrast with the behavior of the baseline  $\kappa$ - $\mu$  shadowed (unimodal) or FTR distributions (only right-bimodality) from which the MFTR distribution originates. This feature brings additional flexibility to improve the versatility of the MFTR model to fit field measurements in emerging wireless scenarios such as mm-Wave and sub-terahertz bands [14].

In Fig. 2, it is confirmed that for low values of  $\Delta$ , i.e., one specular component is dominant in cluster 1, then the MFTR distribution exhibits a unimodal behavior similar to the  $\kappa$ - $\mu$  shadowed case. Conversely, for larger values of  $\Delta$ , i.e., two specular components with similar amplitudes are present in cluster 1, then the MFTR distribution exhibits a bimodal behavior. From Figs. 3-4, we can see that such bimodality of the MFTR distribution is also closely linked to parameters  $m$  and  $K$ . Specifically, large values of  $m$  or  $K$  yield a more pronounced bimodality. Conversely, low values of  $m$  or  $K$  tend to smoothen such bimodality.

<sup>2</sup>The bimodality of the distribution is related to the existence of two local maxima in its PDF.

#### IV. PERFORMANCE ANALYSIS IN WIRELESS SYSTEMS

In this section, we illustrate the flexibility of the MFTR model when used for performance analysis. For exemplary purposes, we analyze key performance metrics such as the outage probability (OP), both in exact and asymptotic forms, as well as the AoF [1].

##### A. Outage Probability

The instantaneous Shannon channel capacity per unit bandwidth is defined as

$$C = \log_2(1 + \gamma). \quad (24)$$

The outage probability is defined as the probability that the capacity  $C$  falls below a certain threshold rate  $R_{th}$ , i.e.,

$$\begin{aligned} P_{out} &= \Pr \{C < R_{th}\} = \Pr \{\log_2(1 + \gamma) < R_{th}\} \\ &= \Pr \left\{ \gamma < \underbrace{2^{R_{th}} - 1}_{\gamma_{th}} \right\}. \end{aligned} \quad (25)$$

Consequently, the OP is given in terms of SNR's CDF as

$$P_{out} = F_\gamma(2^{R_{th}} - 1), \quad (26)$$

in which  $F_\gamma(\cdot)$  is given by either (15), (17) or (21). Although expressed in exact form in terms of the MFTR CDFs previously derived,  $P_{out}$  provides a limited insight concerning the effect of fading parameters on the system performance. Thus, we introduce a closed-form asymptotic OP expression to evaluate the high-SNR regime's system performance below.

##### B. Asymptotic Outage Probability

Here, to get further insights about the role of the fading parameters on system performance, we derive an asymptotic expression to investigate the behavior of the OP given in (26) in the high-SNR regime. Our goal is to obtain an asymptotic expression in the form  $P_{out} \simeq G_c (\gamma_{th}/\bar{\gamma})^{G_d}$  [24], where  $G_c$  and  $G_d$  denote the power offset and the diversity order, respectively. Hence, the corresponding asymptotic OP is given in the following Proposition.

**Proposition 1.** *The asymptotic expression of the OP over MFTR channels can be obtained as*

$$\begin{aligned} P_{out} &\simeq \frac{\mu^{\mu-1}(1+K)^\mu m^m (2^{R_{th}} - 1)^\mu}{\Gamma(\mu)\bar{\gamma}^\mu (m - (\Delta - 1)K\mu)^m} \\ &\quad \times {}_2F_1 \left( 1/2, m; 1; \frac{2\Delta K\mu}{K\mu(1-\Delta) + m} \right). \end{aligned} \quad (27)$$

*Proof.* See Appendix C-A.  $\square$

From (27), notice that the diversity order is linked to the number of multipath waves clusters, i.e.,  $G_d = \mu$ .

### C. Amount of Fading

The AoF is a popular metric used to quantify the severity of fading experienced during transmission under fading channels. It is defined as [1]

$$\text{AoF} = \frac{\mathbb{V}\{\gamma\}}{\mathbb{E}\{\gamma\}^2} = \frac{\mathbb{E}\{\gamma^2\} - \mathbb{E}\{\gamma\}^2}{\mathbb{E}\{\gamma\}^2} = \frac{\mathbb{E}\{\gamma^2\}}{\mathbb{E}\{\gamma\}^2} - 1. \quad (28)$$

Based on (28), a closed-form expression of the AoF is given as stated in the following Proposition.

**Proposition 2.** *Assuming non-constrained arbitrary fading values, a closed-form expression for the AoF over MFTR channels can be formulated as*

$$\begin{aligned} \text{AoF} = & \left(1 - \frac{K^2}{(1+K)^2}\right) \left(1 + \frac{1}{\mu}\right) + \frac{K^2}{(1+K)^2} \\ & \times \left(1 + \frac{1}{m}\right) \left(1 + \frac{\Delta^2}{2}\right) - 1. \end{aligned} \quad (29)$$

*Proof.* See Appendix C-B.  $\square$

## V. NUMERICAL RESULTS

In this section, we provide illustrative numerical results along with MC simulations to verify the analytical performance metrics derived in the previous section by assuming different fading conditions.

Figs. 5 and 6 illustrate the impact of different propagation mechanisms, namely, NLOS- LOS-condition, LOS fluctuation, the existence of one/two dominant components in cluster 1, and clustering of multipath waves, on the OP performance. In both figures, we assume  $K = 15$  and  $R_{\text{th}} = 1$ . Specifically, in Fig. 5, we evaluate the OP vs. the average SNR by varying  $\mu$  and  $m$  for  $\Delta = 0.1$ . From all traces, it can be observed that a contribution of the LOS component with a mild fluctuation ( $m = 10$ ) together with a rich scattering environment ( $\mu = 3$ ) favors the OP performance. Conversely, when both the LOS fluctuation is severe (i.e., lower values of  $m$ ), and a poor scattering condition exists ( $\mu = 1$ ), the OP performance is noticeably reduced. On the other hand, in Fig. 6, we show the OP as a function of the average SNR for different fading values of  $\Delta$  and  $\mu$ , assuming a mild fluctuation ( $m = 5$ ) for the LOS components. Here, we can see that the combination of similar ( $\Delta = 0.9$ ) specular components with many clusters of multipath waves ( $\mu = 4$ ) derives into a better OP behavior. However, in the opposite scenario, i.e., dissimilar ( $\Delta = 0.1$ ) LOS components together with reduced clustering of scattering waves, the OP significantly deteriorates.

Furthermore, in Figs. 5 and 6, we see that the number of clusters of multipath waves contributes directly to the OP slope. This means that the decay in the OP is steeper (i.e., better performance) as the number of scattering wave clusters increases. This is in coherence with the derived diversity order, i.e.,  $G_d = \mu$ .

Fig. 7 shows the effect of the AoF experienced in MFTR fading channels for different fading values, as a function of  $\Delta$ . It becomes clear that the largest AoF occurs for low values of the  $m$ ,  $K$ , and  $\mu$  parameters indicating that the channel is

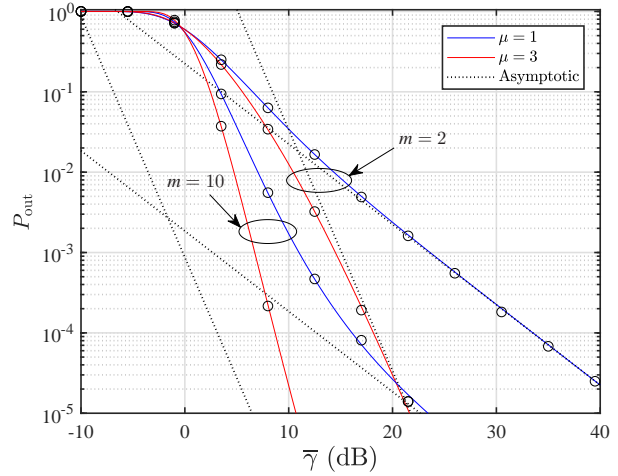


Fig. 5.  $P_{\text{out}}$  as a function of the average SNR, for different values of  $\mu$  and  $m$ . The remaining fading parameters are:  $K = 15$ ,  $\Delta = 0.1$ ,  $R_{\text{th}} = 1$ . Solid lines correspond to the  $P_{\text{out}}$  derived from (26), and dotted lines correspond to the asymptotic  $P_{\text{out}}$  derived from (27). Markers denote MC simulations

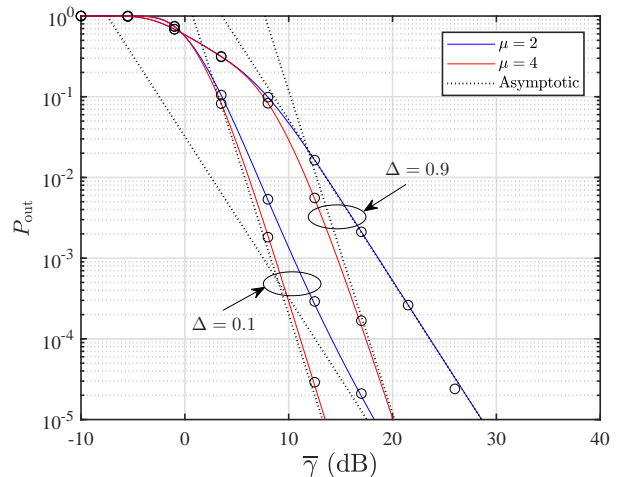


Fig. 6.  $P_{\text{out}}$  as a function of the average SNR, for different values of  $\mu$  and  $\Delta$ . The remaining parameters are:  $K = 15$ ,  $m = 5$ ,  $R_{\text{th}} = 1$ . Solid lines correspond to the  $P_{\text{out}}$  derived from (26), and dotted lines correspond to the asymptotic  $P_{\text{out}}$  derived from (27). Markers denote MC simulations

subject to a more severe multipath fading. Moreover, the AoF increases as the similarity ( $\Delta$ ) between the LOS components becomes large, since partial cancellation between the dominant components becomes more likely as their amplitudes are more balanced.

## VI. CONCLUSIONS

We introduced, for the first time in the literature, a stochastic fading model that combines the key features of ray-based and power envelope-based approaches. This newly proposed fading model unifies and generalizes both the FTR and the  $\kappa$ - $\mu$  shadowed fading models, with a comparable mathematical complexity. The MFTR model captures, through a limited set of physically-meaningful parameters, a number of propagation conditions that appear in many practical scenarios: LOS/NLOS



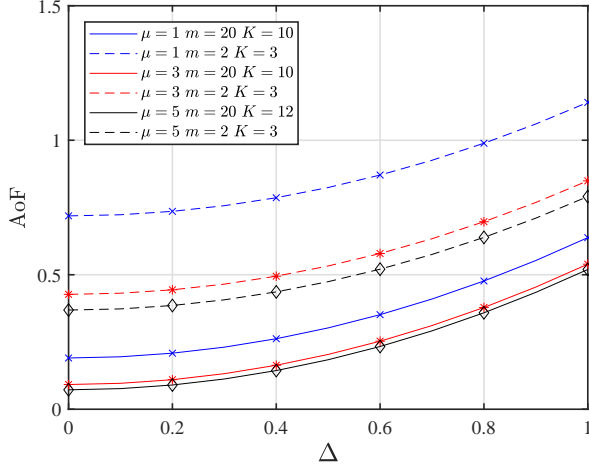


Fig. 7. The AoF vs.  $\Delta$  over MTRF fading channels. Solid lines correspond to the AoF computed via (29) and markers denote Monte Carlo simulations.

power ratio, amplitude imbalances between dominant specular components, random fluctuation of the dominant specular waves, and clustering of multipath waves. In order to facilitate its use for performance analysis purposes, alternative expressions for its statistics are derived, which enable us to express the desired performance metric under MTRF fading directly from those available either for  $\kappa$ - $\mu$  shadowed or Nakagami- $m$  fading. All these features make the MTRF model a strong contender to being the most generalized and comprehensive fading channel model in the state-of-the-art up to the present date.

#### APPENDIX A PROOF OF LEMMA 1

Departing from a generalized physical cluster-based model [7, 8], let us consider a compact form expression for the signal power,  $W$ , given by

$$W = \sum_{i=1}^{\mu} \left| Z_i + \sqrt{\zeta} p_i \right|^2, \quad (30)$$

where  $\mu$  is the number of clusters,  $Z_i = X_i + jY_i$  with  $X_i$  and  $Y_i$  being independent Gaussian RVs with zero-mean and variance  $\sigma^2$ , i.e.,  $X_i, Y_i \sim \mathcal{N}(0, \sigma^2)$ , representing the  $i$ th cluster of scattering waves, and  $\zeta$  denotes the fluctuation of the LOS component, which is statistically distributed as a unit-mean gamma RV with shape parameter  $m$ . On the other hand, in purely cluster-based models, the total power of the dominant components can be distributed indistinctly throughout the clusters. Here, without loss of generality, we assume that the total power coming from two specular components is allocated in cluster 1, so no dominant specular components are found in the remaining clusters. With this in mind, the dominant specular component, denoted by  $p_i$ , of the  $i$ th cluster can be expressed as

$$p_i = \begin{cases} 0, & \text{for } \forall i > 1 \\ V_1 e^{j\phi_1} + V_2 e^{j\phi_2} = e^{j\phi_1} (V_1 + V_2 e^{j\alpha}), & \text{for } i = 1, \end{cases} \quad (31)$$

in which  $V_n \exp(j\phi_n)$  for  $n = \{1, 2\}$  denote the  $n$ th specular component with constant amplitude  $V_n$  and a uniformly distributed random phase, such that,  $\phi_n \sim \mathcal{U}(0, 2\pi)$ . Moreover,  $\alpha = \phi_2 - \phi_1$  is the phase difference between the two LOS components. Given that  $\phi_n \sim \mathcal{U}(0, 2\pi)$  and because of the modulo  $2\pi$  operation, it follows that,  $\alpha \sim \mathcal{U}(0, 2\pi)$  [13].

Let us consider the channel model given in (30) conditioned to a particular realization  $\alpha = \theta$  of the RV characterizing the phase difference between the two LOS components in cluster 1. Then, (30) can be seen as a  $\kappa$ - $\mu$  shadowed distributed RV for a given  $\theta$ , where  $|p_1|$  is now constant (i.e., deterministic) and no longer arbitrarily distributed. Based on this, the mean power of the dominant components for the underlying  $\kappa$ - $\mu$  shadowed RV in (30), conditioned on  $\theta$ , i.e.,  $d_\theta^2 \triangleq d^2|_{\alpha=\theta}$  is given by

$$d_\theta^2 = |p_1|^2 = |V_1 + V_2 e^{j\theta}|^2 = V_1^2 + V_2^2 + 2V_1 V_2 \cos \theta. \quad (32)$$

With the help of (32), the ratio between the total power of the dominant components and the total power of the scattered waves, conditioned on  $\theta$  can be formulated as

$$\kappa_\theta = \frac{d_\theta^2}{2\sigma^2\mu}. \quad (33)$$

The conditional average SNR for the fading model described in (30) will be

$$\begin{aligned} \bar{\gamma}_\theta &= \frac{\bar{\gamma}}{\Omega} \mathbb{E}\{W_\theta\} = \frac{\bar{\gamma}}{\Omega} (V_1^2 + V_2^2 + 2V_1 V_2 \cos \theta + 2\sigma^2\mu) \\ &= \frac{\bar{\gamma}}{\Omega} 2\sigma^2\mu(1 + \kappa_\theta). \end{aligned} \quad (34)$$

Similarly, from (6) we can compute the mean power of the dominant components for the MTRF model, conditioned on  $\theta$ . Thus, we have

$$\begin{aligned} d_{\theta, \text{MTRF}}^2 &= (V_1 \cos \phi_1 + V_2 \cos \phi_2)^2 + (V_1 \sin \phi_1 + V_2 \sin \phi_2)^2 \\ &= V_1^2 + V_2^2 + 2V_1 V_2 \cos(\phi_2 - \phi_1) \\ &= V_1^2 + V_2^2 + 2V_1 V_2 \cos \theta. \end{aligned} \quad (35)$$

It is evident that the parameters in (32) and (35), related to the  $\kappa$ - $\mu$  shadowed and MTRF models, respectively, are equivalent. Hence, with the above definitions, we are ready to find an insightful connection between the  $\kappa$ - $\mu$  shadowed and the MTRF models. To accomplish this, by inserting (7), (8) and (35) into (33), we get

$$\begin{aligned} \kappa_\theta &= \frac{V_1^2 + V_2^2 + 2V_1 V_2 \cos \theta}{2\sigma^2\mu} = \frac{(V_1^2 + V_2^2)(1 + \Delta \cos \theta)}{2\sigma^2\mu} \\ &= K(1 + \Delta \cos \theta). \end{aligned} \quad (36)$$

Note that from (9) and (34) we can write, respectively

$$\frac{1 + K}{\bar{\gamma}} = \frac{1}{\frac{\bar{\gamma}}{\Omega} 2\sigma^2\mu}, \quad (37)$$

$$\frac{1 + \kappa_\theta}{\bar{\gamma}_\theta} = \frac{1}{\frac{\bar{\gamma}}{\Omega} 2\sigma^2\mu}, \quad (38)$$

and equating (37) and (38), it is clear that

$$\frac{1 + \kappa_\theta}{\bar{\gamma}_\theta} = \frac{1 + K}{\bar{\gamma}}. \quad (39)$$

Here, we point out that with the aid of the key findings in (36) and (39), we can derive the MGF of the MFTR model from the conditional MGF of the  $\kappa$ - $\mu$  shadowed, which is given by

$$M_{\gamma|\theta}^{\kappa\mu s}(s) = \frac{\left(1 - \frac{\bar{\gamma}_\theta}{\mu(1+\kappa_\theta)}s\right)^{m-\mu}}{\left(1 - \frac{\mu\kappa_\theta+m}{m} \frac{\bar{\gamma}_\theta}{\mu(1+\kappa_\theta)}s\right)^m} \quad (40)$$

Now, taking into account (36) and (39) into (40), yields

$$M_{\gamma|\theta}^{\kappa\mu s}(s) = \frac{m^m \mu^\mu (1+K)^\mu (\mu(1+K) - \bar{\gamma}s)^{m-\mu}}{(a(s) + b(s) \cos \theta)^m} \quad (41)$$

where, we have defined

$$a(s) = m\mu(1+K) - (\mu K + m)\bar{\gamma}s, \quad b(s) = -\mu K \Delta \bar{\gamma}s. \quad (42)$$

The MGF of the SNR of the MFTR model can be obtained by averaging (41) with respect to the RV<sup>3</sup>  $\theta$ , i.e.,

$$M_\gamma(s) = \frac{m^m \mu^\mu (1+K)^\mu}{(\mu(1+K) - \bar{\gamma}s)^{\mu-m}} \frac{1}{\pi} \underbrace{\int_0^\pi \frac{d\theta}{(a(s) + b(s) \cos \theta)^m}}_{I_1}, \quad (43)$$

Using [25, Eq. (3.661.4)],  $I_1$  can be evaluated in exact closed-form; thus (10) is obtained, in which  $\mathcal{R}(\mu, m, K, \Delta; s) = [a(s)]^2 - [b(s)]^2$ . This completes the proof.

## APPENDIX B PROOFS OF LEMMAS 2 AND 4

### A. Proof of Lemma 2

Notice that the  $\mathcal{R}(\mu, m, K, \Delta; s)$  polynomial within the MGF given in (10) can be factored as

$$\begin{aligned} \mathcal{R}(\mu, m, K, \Delta; s) &= [(1+K)m\mu - (m + \mu K(1 + \Delta))\bar{\gamma}s] \\ &\times [(1+K)m\mu - (m + \mu K(1 - \Delta))\bar{\gamma}s]. \end{aligned} \quad (44)$$

For the sake of mathematical legibility, we define the following ancillary terms

$$\begin{aligned} a_1 &= \frac{(1+K)m\mu}{(m + \mu K)\bar{\gamma}}, & a_2 &= \frac{(1+K)m\mu}{(m + \mu K(1 + \Delta))\bar{\gamma}}, \\ a_3 &= \frac{(1+K)m\mu}{(m + \mu K(1 - \Delta))\bar{\gamma}}, & a_4 &= \frac{(1+K)\mu}{\bar{\gamma}}. \end{aligned} \quad (45)$$

Inserting (12) together with (44)-(45) into (10), the MGF of the MFTR model with  $m \in \mathbb{Z}^+$  can be rewritten as

$$\begin{aligned} M_\gamma(s) &= \frac{(a_2 a_3)^{m/2}}{\Gamma(\mu) 2^{m-1} a_4^{m-\mu}} \sum_{q=0}^{\lfloor \frac{m-1}{2} \rfloor} \frac{C_q^{m-1}}{(-1)^{-q}} \left[ \frac{\sqrt{a_2 a_3}}{a_1} \right]^{m-1-2q} \\ &\times \frac{\Gamma(\mu)}{s^\mu} \left(1 - \frac{a_1}{s}\right)^{m-1-2q} \left(1 - \frac{a_2}{s}\right)^{\frac{1}{2}+q-m} \\ &\times \left(1 - \frac{a_3}{s}\right)^{\frac{1}{2}+q-m} \left(1 - \frac{a_4}{s}\right)^{m-\mu}. \end{aligned} \quad (46)$$

Finally, the PDF is obtained straightforwardly from this MGF through the inverse Laplace transform (LT), i.e.,  $f_\gamma(x) = \mathcal{L}^{-1}[M_\gamma(-s); x]$ ; thus, (14) arises from (46) with the help of the LT pair given in [19, Eq. (4.24.3)]. Similarly, (15) is obtained by considering that  $F_\gamma(x) = \mathcal{L}^{-1}[M_\gamma(-s)/s; x]$ .

<sup>3</sup>Recall that  $\frac{1}{2\pi} \int_0^{2\pi} f(\theta) d\theta \equiv \frac{1}{\pi} \int_0^\pi f(\theta) d\theta$  because the integrand is symmetric with respect to  $\pi$ .

### B. Proof of Lemma 4

Many distributions in the literature of wireless channel modeling can be expressed in terms of a mixture of Gamma distributions, either in exact [26] or approximate form [27]. On this basis, we aim to express the MFTR's statistics as a mixture of Gamma distributions. To do this, we start from the exact expression of the  $\kappa$ - $\mu$  shadowed model as an infinite mixture of Gamma distributions [28, eq. 25]. Hence, the statistics of the MFTR distribution when conditioned on  $\theta$  are those of the  $\kappa$ - $\mu$  shadowed model, so that the PDF and CDF can be given as:

$$f_{\gamma|\theta}^{\kappa\mu s}(x) = \sum_{i=0}^{\infty} w_i |\theta| f_X^G \left( \mu + i; \frac{(\mu + i)\bar{\gamma}_\theta}{\mu(1 + \kappa_\theta)}; x \right), \quad (47)$$

$$F_{\gamma|\theta}^{\kappa\mu s}(x) = \sum_{i=0}^{\infty} w_i |\theta| F_X^G \left( \mu + i; \frac{(\mu + i)\bar{\gamma}_\theta}{\mu(1 + \kappa_\theta)}; x \right), \quad (48)$$

where the PDF and CDF of the Gamma distribution were defined in (19), and the conditional mixture coefficients are given by

$$w_i |\theta| = \frac{\Gamma(m+i)(\mu\kappa_\theta)^i m^m}{\Gamma(m)\Gamma(i+1)(\mu\kappa_\theta + m)^{m+i}}. \quad (49)$$

Applying the connection between the  $\kappa$ - $\mu$  shadowed and the MFTR models as shown in (36) and (39), the PDF and CDF distributions of the MFTR model are formulated after averaging over the distribution of  $\theta$  as

$$f_\gamma(x) = \sum_{i=0}^{\infty} w_i f_X^G \left( \mu + i; \frac{(\mu + i)\bar{\gamma}}{\mu(1 + \kappa)}; x \right), \quad (50)$$

$$F_\gamma(x) = \sum_{i=0}^{\infty} w_i F_X^G \left( \mu + i; \frac{(\mu + i)\bar{\gamma}}{\mu(1 + \kappa)}; x \right), \quad (51)$$

where now the weighting coefficients,  $w_i$ , are rewritten as

$$\begin{aligned} w_i &= \frac{\Gamma(m+i)(\mu K)^i m^m}{\Gamma(m)\Gamma(i+1)} \\ &\times \frac{1}{\pi} \underbrace{\int_0^\pi \frac{(1 + \Delta \cos \theta)^i}{(\mu K(1 + \Delta \cos \theta) + m)^{m+i}} d\theta}_{I_2}. \end{aligned} \quad (52)$$

Using the results in the Appendix of [22],  $I_2$  can be evaluated in closed-form fashion as

$$\begin{aligned} I_2 &= \frac{(1-\Delta)^i}{\sqrt{\pi}(\mu K(1-\Delta)+m)^{m+i}} \sum_{q=0}^i \binom{i}{q} \frac{\Gamma(q+\frac{1}{2})}{\Gamma(q+1)} \left(\frac{2\Delta}{1-\Delta}\right)^q \\ &\times {}_2F_1 \left( m + i, q + \frac{1}{2}; q + 1; \frac{-2\mu K \Delta}{\mu K(1-\Delta)+m} \right), \end{aligned} \quad (53)$$

when  $m$  is an arbitrary real number. Then, by substituting (53) into (52) and then combining the resulting expression with (50) and (51), the PDF and CDF of the MFTR model for arbitrary values can be expressed as in (16) and (17), respectively. This completes the proof.

APPENDIX C  
PROOFS OF PROPOSITIONS 1, AND 2

A. Asymptotic Outage Probability

In order to derive the asymptotic outage probability, we take advantage of the connections between the  $\kappa$ - $\mu$  shadowed and the MFTR models obtained in Appendix A. For this purpose, we start from the conditional<sup>4</sup> $\kappa$ - $\mu$  shadowed asymptotic CDF, given by [29, Eq. (35)]

$$F_{\gamma|\theta}^{\kappa\mu s}(x) \simeq \frac{\mu^{\mu-1}(1+\kappa_\theta)^\mu m^m}{(\kappa_\theta\mu+m)^m \Gamma(\mu)} \left(\frac{x}{\bar{\gamma}_\theta}\right)^\mu. \quad (54)$$

Next, using the relationships between the  $\kappa$ - $\mu$  shadowed and the MFTR models given in (36) and (39) into (54), we get

$$F_{\gamma|\theta}^{\kappa\mu s}(x) \simeq \frac{\mu^{\mu-1}(1+K)^\mu m^m}{\Gamma(\mu)} \left(\frac{x}{\bar{\gamma}}\right)^\mu \times \underbrace{\frac{1}{\pi} \int_0^\pi \frac{1}{(\mu K(1+\Delta \cos \theta) + m)^m} d\theta}_{I_3}. \quad (55)$$

Employing [30, eq. (38)], the integral in  $I_3$  can be expressed in simple exact closed-form as

$$I_3 = (m - (\Delta - 1)K\mu)^{-m} \times {}_2F_1\left(\frac{1}{2}, m; 1; \frac{2\Delta K\mu}{K\mu(1-\Delta) + m}\right) \quad (56)$$

Substituting (56) into (55), the MFTR asymptotic CDF is attained as

$$F_\gamma(x) \simeq \frac{\mu^{\mu-1}(1+K)^\mu m^m}{(m - (\Delta - 1)K\mu)^m \Gamma(\mu)} \left(\frac{\gamma}{\bar{\gamma}}\right)^\mu \times {}_2F_1\left(\frac{1}{2}, m; 1; \frac{2\Delta K\mu}{K\mu(1-\Delta) + m}\right). \quad (57)$$

Finally, taking into account that  $P_{\text{out}} \simeq F_\gamma(2^{R_{\text{th}}} - 1)$  with  $F_\gamma(\cdot)$  given in (57), the asymptotic outage probability can be reached as in (27), which concludes the proof.

B. AoF

Similar to the methodology described in Appendix C-A, we calculate the AoF of the MFTR model from the conditional second moment of the  $\kappa$ - $\mu$  shadowed distribution, which is given by [31, Eq. (3.10)]

$$\mathbb{E}\left\{\gamma_{|\theta}^2\right\}^{\kappa\mu s} = \frac{\bar{\gamma}_\theta^2 (m(1+\mu)(1+2\kappa_\theta) + \mu\kappa_\theta^2(1+m))}{m\mu(1+\kappa_\theta)^2} \quad (58)$$

Then, using the connections between the  $\kappa$ - $\mu$  shadowed and the MFTR models obtained in (36) and (39) into (58), the second moment of the MFTR model is expressed as

$$\mathbb{E}\left\{\gamma^2\right\} = \frac{\bar{\gamma}^2 (m(1+\mu)(1+2\mathbb{E}\{\kappa_\theta\}) + \mu\mathbb{E}\{\kappa_\theta^2\}(1+m))}{m\mu(1+K)^2} \quad (59)$$

<sup>4</sup>In practice, it suffices to replace  $\bar{\gamma}$  and  $\kappa$  by  $\bar{\gamma}_\theta$  and  $\kappa_\theta$ , respectively, in the original  $\kappa$ - $\mu$  shadowed asymptotic CDF, as indicated in Appendix A.

where

$$\mathbb{E}\{\kappa_\theta\} = \frac{1}{\pi} \int_0^\pi K(1 + \Delta \cos \theta) d\theta = K, \quad (60)$$

and

$$\mathbb{E}\{\kappa_\theta^2\} = \frac{1}{\pi} \int_0^\pi (K(1 + \Delta \cos \theta))^2 d\theta = K^2 \left(1 + \frac{\Delta^2}{2}\right). \quad (61)$$

Substituting (60) and (61) into (59) yields

$$\mathbb{E}\left\{\gamma^2\right\} = \frac{\bar{\gamma}^2}{m\mu(1+K)^2} \left( m(1+\mu)(1+2K) + \mu K^2 \times \left(1 + \frac{\Delta^2}{2}\right)(1+m) \right). \quad (62)$$

Finally, inserting (62) together with  $\mathbb{E}\{\gamma\}^2 = \bar{\gamma}^2$  into (28) and after some algebraic manipulations, the AoF of the MFTR model can be attained as in (29). This completes the proof.

REFERENCES

- [1] M. K. Simon and M.-S. Alouini, *Digital communication over fading channels*. Wiley-IEEE Press, 2005.
- [2] P. Beckmann, "Statistical distribution of the amplitude and phase of a multiply scattered field," *J. Res. Natl. Bur. Stand. (U. S.)-D. Radio Propagation*, vol. 66D, no. 3, pp. 231–240, 1962.
- [3] J. M. Romero-Jerez, F. J. Lopez-Martinez, J. F. Paris, and A. J. Goldsmith, "The fluctuating two-ray fading model: Statistical characterization and performance analysis," *IEEE Trans. Wireless Commun.*, vol. 16, no. 7, pp. 4420–4432, 2017.
- [4] T. R. R. Marins, A. A. dos Anjos, V. M. R. Peñarrocha, L. Rubio, J. Reig, R. A. A. de Souza, and M. D. Yacoub, "Fading evaluation in the mm-Wave band," *IEEE Trans. Commun.*, vol. 67, no. 12, pp. 8725–8738, 2019.
- [5] P. C. F. Eggers, M. Angelichinoski, and P. Popovski, "Wireless channel modeling perspectives for ultra-reliable communications," *IEEE Trans. Wireless Commun.*, vol. 18, no. 4, pp. 2229–2243, 2019.
- [6] N. Mehrnia and S. Coleri, "Wireless channel modeling based on extreme value theory for ultra-reliable communications," *IEEE Trans. Wireless Commun.*, vol. 21, no. 2, pp. 1064–1076, 2022.
- [7] M. D. Yacoub, "The  $\kappa$ - $\mu$  distribution and the  $\eta$ - $\mu$  distribution," *IEEE Antennas Propagat. Mag.*, vol. 49, no. 1, pp. 68–81, 2007.
- [8] J. F. Paris, "Statistical characterization of  $\kappa$ - $\mu$  shadowed fading," *IEEE Trans. Veh. Technol.*, vol. 63, no. 2, pp. 518–526, 2014.
- [9] L. Moreno-Pozas, F. J. Lopez-Martinez, J. F. Paris, and E. Martos-Naya, "The  $\kappa$ - $\mu$  shadowed fading model: Unifying the  $\kappa$ - $\mu$  and  $\eta$ - $\mu$  distributions," *IEEE Trans. Veh. Technol.*, vol. 65, no. 12, pp. 9630–9641, 2016.
- [10] G. D. Durgin, *Theory of stochastic local area channel modeling for wireless communications*. PhD thesis, Virginia Polytechnic Institute and State University, 2000.
- [11] J. M. Romero-Jerez, F. J. Lopez-Martinez, J. P. Peña Martin, and A. Abdi, "Stochastic fading channel models with multiple dominant specular components," *IEEE Trans. Veh. Technol.*, vol. 71, no. 3, pp. 2229–2239, 2022.
- [12] G. Durgin, T. Rappaport, and D. de Wolf, "New analytical models and probability density functions for fading in wireless communications," *IEEE Trans. Commun.*, vol. 50, no. 6, pp. 1005–1015, 2002.
- [13] M. Rao, F. J. Lopez-Martinez, M.-S. Alouini, and A. Goldsmith, "MGF approach to the analysis of generalized two-ray fading models," *IEEE Trans. Wireless Commun.*, vol. 14, no. 5, pp. 2548–2561, 2015.
- [14] H. Du, J. Zhang, K. Guan, D. Niyato, H. Jiao, Z. Wang, and T. Kuerner, "Performance and optimization of reconfigurable intelligent surface aided THz communications," *IEEE Trans. Commun.*, vol. 70, no. 5, pp. 3575–3593, 2022.
- [15] T. Mavridis, L. Petrillo, J. Sarrazin, A. Benlarbi-Delai, and P. De Doncker, "Near-body shadowing analysis at 60 GHz," *IEEE Trans. Antennas Propag.*, vol. 63, no. 10, pp. 4505–4511, 2015.

- [16] S. K. Yoo, S. L. Cotton, P. C. Sofotasios, and S. Freear, "Shadowed fading in indoor off-body communication channels: A statistical characterization using the  $\kappa$ - $\mu$  /gamma composite fading model," *IEEE Trans. Commun.*, vol. 15, no. 8, pp. 5231–5244, 2016.
- [17] A. Abdi, W. Lau, M.-S. Alouini, and M. Kaveh, "A new simple model for land mobile satellite channels: first- and second-order statistics," *IEEE Trans. Wireless Commun.*, vol. 2, no. 3, pp. 519–528, 2003.
- [18] M. Abramowitz and I. A. Stegun, *Handbook of Mathematical Functions With Formulas, Graphs, and Mathematical Tables*. US Dept. Of Commerce, National Bureau Of Standards, Washington DC, 10th ed., 1972.
- [19] P. W. Karlsson and H. M. Srivastava, *Multiple Gaussian Hypergeometric Series*. John Wiley & Sons, 1985.
- [20] Y. A. Brychkov and N. Saad, "Some formulas for the appell function  $F_1(a, b, b'; c; w, z)$ ," *Integral Transforms and Special Functions*, vol. 23, no. 11, pp. 793–802, 2012.
- [21] E. Martos-Naya, J. M. Romero-Jerez, F. J. Lopez-Martinez, and J. F. Paris, "A matlab program for the computation of the confluent hypergeometric function  $\Phi_2$ ," 2016. [Online]. Available: <https://riuma.uma.es/xmlui/handle/10630/12068>.
- [22] M. Olyaei, J. M. Romero-Jerez, F. J. Lopez-Martinez, and A. J. Goldsmith, "Alternative formulations for the fluctuating two-ray fading model," *IEEE Trans. Wireless Commun. (Early Access)*, 2022.
- [23] F. Weinstein, "Simplified relationships for the probability distribution of the phase of a sine wave in narrow-band normal noise (corresp.)," *IEEE Trans. Inf. Theory*, vol. 20, no. 5, pp. 658–661, 1974.
- [24] Z. Wang and G. Giannakis, "A simple and general parameterization quantifying performance in fading channels," *IEEE Trans. Commun.*, vol. 51, no. 8, pp. 1389–1398, 2003.
- [25] I. S. Gradshteyn and I. M. Ryzhik, *Table of Integrals, Series and Products*. San Diego, CA, USA: Academic Press, 2007.
- [26] N. Y. Ermolova, "Capacity analysis of two-wave with diffuse power fading channels using a mixture of gamma distributions," *IEEE Commun. Lett.*, vol. 20, no. 11, pp. 2245–2248, 2016.
- [27] M. Wiper, D. R. Insua, and F. Ruggeri, "Mixtures of gamma distributions with applications," *J. Comput. Graph. Statist.*, vol. 10, no. 3, pp. 440–454, 2001.
- [28] P. Ramirez-Espinosa and F. Javier Lopez-Martinez, "Composite fading models based on inverse gamma shadowing: Theory and validation," *IEEE Trans. Wireless Commun.*, pp. 1–1, 2021.
- [29] U. Fernandez-Plazaola, L. Moreno-Pozas, F. J. Lopez-Martinez, J. F. Paris, E. Martos-Naya, and J. M. Romero-Jerez, "A tractable product channel model for line-of-sight scenarios," *IEEE Trans. Wireless Commun.*, vol. 19, no. 3, pp. 2107–2121, 2020.
- [30] C. Garcia-Corrales, U. Fernandez-Plazaola, F. J. Canete, J. F. Paris, and F. J. Lopez-Martinez, "Unveiling the hyper-rayleigh regime of the fluctuating two-ray fading model," *IEEE Access*, vol. 7, pp. 75367–75377, 2019.
- [31] C. Garcia Corrales, *Análisis de Prestaciones en Canales con Desvanecimientos de Tipo  $\kappa$ - $\mu$  shadowed*. PhD thesis, Departamento de Ingeniería de Comunicaciones, Universidad de Málaga, 2021.